

Online Miniaturized Asymmetrical Flow Field-Flow Fractionation and Inductively Coupled Plasma Mass Spectrometry for Metalloprotein Analysis of Plasma from Patients with Lung Cancer

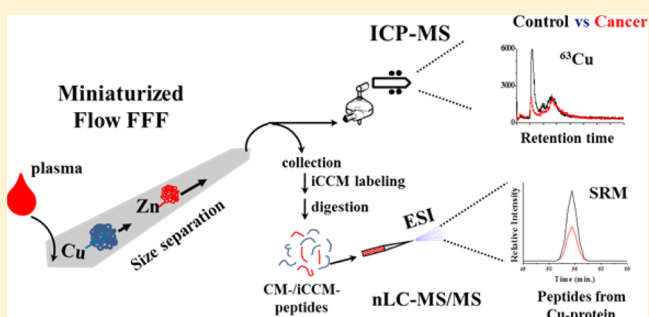
Jin Yong Kim,[†] Heung Bin Lim,^{*,‡} and Myeong Hee Moon^{*,†}

[†]Department of Chemistry, Yonsei University, Seoul, 03722, Korea

[‡]Department of Chemistry, Dankook University, Yongin-si, Gyeonggi-do 16890, Korea

Supporting Information

ABSTRACT: Metalloproteins (metal-binding proteins) refer to proteins containing metal ion cofactors. The importance of these proteins has increased owing to their involvement in many biological processes. Here, we introduce an analytical platform based on online coupling of miniaturized asymmetrical flow field-flow fractionation (mAF4) and inductively coupled plasma mass spectrometry (ICPMS) for size separation of proteins followed by the detection of metals associated with plasma metalloproteins. Not only did the mild separation of mAF4 get carried out in a biological buffer solution to minimize disruption of the metal-complex structure but free metal ions and salts from complicated biological samples were also removed during separation by crossflow. The relative quantities of metalloproteins detected by mAF4-ICPMS between plasma samples from patients with lung cancer and healthy controls were compared by determining the peak areas of detected elements and retention times; among these, 7 (⁵⁵Mn, ⁶⁰Ni, ⁶³Cu, ⁶⁶Zn, ⁹⁰Zr, ¹²⁷I, and ¹³⁷Ba) out of 16 elements showed substantial changes in patients with lung cancer. For the quantitative comparison of metalloproteins, protein fractions during mAF4 were collected and analyzed by nanoflow liquid chromatography–tandem mass spectrometry using isotope-coded carbamidomethylation. Quantitative analysis showed that some metalloproteins associated with ⁵⁵Mn, ⁶⁰Ni, ⁶³Cu, and ⁶⁶Zn exhibited changes similar to those in patients. These findings demonstrated the potential of mAF4-ICPMS as a powerful high-speed screening method for targeted metalloproteins related to diseases.



Metalloproteins (metal-binding proteins) account for approximately one-third of all proteins found in nature.^{1,2} By binding with proteins, metals in biological systems play crucial roles in respiration, storage/transportation of proteins, and signal transduction. Although metals are present at trace levels, imbalances in metal concentration or lack of essential metals may alter the function and structure of proteins through loss of stabilization, resulting in disease onset.³ Recent reports have shown that particular metals may be imbalanced in biological systems in the context of several diseases, including Alzheimer's disease (increased levels of copper, iron, and zinc in amyloid plaques),^{4,5} Huntington's disease (iron accumulated in neurons),⁶ Wilson and Menkes disease (copper),⁷ atherosclerosis (iron and copper elevated in atherosclerotic plaques),⁸ and prostate cancer (iron, copper, nickel, and magnesium elevated in malignant tissue).⁹ A study of the molecular and cellular mechanisms of metal ions showed that chromium may provide beneficial effects in alleviating insulin resistance found in type 2 diabetes.¹⁰ Moreover, exposure to certain carcinogenic metals, such as arsenic, cadmium, cobalt, chromium, and nickel, have long been known to increase cancer incidence.^{11,12}

Although detailed analyses are necessary to understand the functions of metalloproteins in relation to diseases, such studies

require that the original structure of metal–metalloprotein complexes be maintained intact and that matrix interference be minimized without losing detection sensitivity.¹⁶ Because metalloproteins in biological systems are complex and exhibit low metal concentrations, analysis of metals in metalloproteins has been made possible by the use of inductively coupled plasma mass spectrometry (ICPMS),^{13–16} which provides robust, highly sensitive detection of metals, and information regarding isotopes. Most of these studies have been carried out using separation methods, such as capillary electrophoresis (CE),^{17,18} size exclusion chromatography (SEC),^{19,20} reversed phase liquid chromatography (RPLC),^{21,22} anion exchange chromatography (AEC),^{23,24} and hydrophilic interaction chromatography (HILIC),²⁵ combined with ICPMS. However, chromatographic separation may induce loss of metalloproteins from unwanted interactions with packing materials or possible dissociation of metals from metalloprotein complexes due to structural deformations in organic solvents.

Received: July 20, 2016

Accepted: September 17, 2016

Published: September 17, 2016

Flow field-flow fractionation (FIFFF) can be used as an alternative separation method with online coupling to ICPMS for the size-based separation of intact metalloproteins in aqueous solutions and simultaneous metal analysis. FIFFF, a variant of field-flow fractionation (FFF), is an elution-based method employing an unobstructed channel to separate macromolecules by using two flow streams (migration flow in the axial direction of the channel and crossflow moving across the rectangular or cylindrical channel space).^{26,27} Sample components in the FIFFF channel are driven toward the vicinity of a channel wall by crossflow and simultaneously protrude away from the wall by diffusion. Therefore, smaller diameter molecules having more rapid diffusion are placed at an equilibrium position higher from the channel wall than larger molecules; thus, they migrate faster than larger molecules when a migration flow with a parabolic flow velocity profile is applied. Since separation in FIFFF does not rely on a partition or an interaction of sample components with the packing materials and utilizes biological buffer solution, it is possible to maintain intact conditions of biological species with the minimization of shear-induced degradation or deformation. FIFFF has been applied to a variety of biological macromolecules, such as proteins, cells, subcellular species, exosomes, and lipoproteins.^{28–35} Moreover, a miniaturized asymmetrical FIFFF (mAF4) channel can be directly interfaced to electrospray ionization-mass spectrometry (ESI-MS) for the top-down analysis of size-fractionated proteins or plasma lipoproteins (lipid analysis) due to reduction of the outflow rate down to few $\mu\text{L}/\text{min}$, which is beneficial for ESI-MS.^{36,37}

Online coupling of FFF with ICPMS has been introduced with sedimentation FFF (SdFFF) for river suspended matter³⁸ and with FIFFF for colloidal materials,³⁹ showing excellent capacity for determination of the particle size-dependent distribution of metal species. Most FFF-ICPMS studies have focused on environmental colloids and inorganic nanoparticles,^{40,41} with the exception of a feasibility study of FIFFF-ICPMS for few metal-containing protein standards⁴² and a recent approach to detect wear metal particles in hip aspirate samples from patients who have undergone hip replacement.⁴³ The latter also demonstrated the possibility of detecting few metals in patient serum samples, but was limited to metals released from particles associated with highly abundant proteins compared with retention times of standard albumin and transferrin. However, difficulties in the detection of low-abundance metalloproteins have arisen from the use of conventional AF4 channels because they are often operated at a few tenths to 1 mL/min, which must be split when combined with ICPMS.

In this study, we introduce an integrated approach to analyze metalloproteins by online coupling of mAF4 with ICPMS for the separation of the plasma proteome (depleted of the two high-abundance proteins albumin and IgG) followed by metal detection in metal-binding proteins and nanoflow liquid chromatography–tandem mass spectrometry (nLC–ESI-MS/MS) for quantitative analysis of metalloproteins. By employing mAF4, the outflow rate was reduced to a few $\mu\text{L}/\text{min}$, which was suitable for direct feeding to ICPMS. Moreover, this method had several advantages, including minimization of the disruption of metal-complex structures through the use of a buffer solution and removal of free metal ions and salts from complicated biological samples during separation. mAF4-ICPMS was applied for the relative quantification of 14 metals and 2 halogens from human plasma samples collected from

patients with lung cancer in comparison with those of healthy controls. For quantitative proteomic analysis of metalloproteins, protein fractions were collected during mAF4 separation and were quantified by nLC–ESI-MS/MS using selected reaction monitoring (SRM) based on the isotope coded carbamidomethylation (iCCM) method⁴⁴ in which the thiol group of the Cys residue in the protein was reacted with isotopic iodoacetamide (IAA; 4 Da difference between light and heavy labeling). The relative changes in metalloproteins in serum samples from patients with lung cancer were compared with the changes of associated metals that were found to have significant differences from AF4-ICPMS experiments.

EXPERIMENTAL SECTION

Materials and Reagents. Ammonium bicarbonate (NH_4HCO_3), six protein standards (carbonic anhydrase, transferrin, alcohol dehydrogenase, ferritin, thyroglobulin, and glutathione peroxidase), dithiothreitol, urea, IAA ($\text{C}_2\text{H}_4\text{INO}$), heavy IAA (IAA*, $^{13}\text{C}_2\text{H}_2\text{D}_2\text{INO}$), L-cysteine, phosphate-buffered saline (PBS), and the ProteoPrep Immunoaffinity Albumin & IgG Depletion Kit were purchased from Sigma-Aldrich (St. Louis, MO). Sequencing-grade trypsin and Lys C were from Promega Corp. (Madison, WI). Fused-silica capillaries (25, 50, 75, and 100 μm i.d.; 365 μm o.d. for all), which were used for preparing the capillary LC column, trapping column, and tubing connections, were obtained from Polymicro Technology LCC (Phoenix, AZ). For column packing, Magic C18AQ beads (3 μm –100 Å and 3 μm –200 Å) were purchased from Michrom Bioresources, Inc. (Auburn, CA). All fittings, adapters, and PEEK tubing for nLC were purchased from Upchurch Scientific of IDEX Health & Science, LCC (Oak Harbor, WA). High-performance liquid chromatography (HPLC)-grade water and acetonitrile for nLC were from J. T. Baker (Deventer, The Netherlands). Plasma samples from 10 patients with lung cancer and 10 healthy controls were obtained with approval of the Institutional Review Board (IRB) from Severance Hospital Gene Bank (Seoul, Korea). Plasma samples were treated with a ProteoPrep Immunoaffinity depletion kit to deplete albumin and IgG prior to analysis, and the protein concentration of each depleted plasma sample was measured using Bradford assays with Bradford reagent from Bio-Rad Laboratories, Inc. (Hercules, CA).

mAF4-ICPMS. The mAF4 channel utilized in this study (see Figure 1) was assembled as described in a previous work,⁴⁵

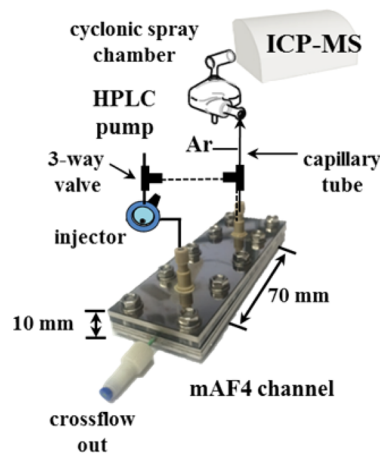


Figure 1. Online mAF4-ICPMS system.

except that both the 1.5 mm-thick top block and the acrylic depletion wall of the channel were replaced with thicker materials (3 mm-thick stainless steel plate and 2.5 mm-thick acrylic plate, respectively) to prevent from deformation. Since Teflon tubing (0.010 in. i.d. and 1/16 in. o.d.) was inserted at the bottom of acrylic plate through a 10-32 Coned Nanoport Assembly from Upchurch Scientific, a direct contact between carrier liquid including sample components and metallic part was avoided. The channel bottom block was stacked with two 1.5 mm-thick SS plates; one of the plates was embedded with a 1.5 mm-thick SS frit (10 cm × 1.5 cm × 0.15 cm, 5 μm pore size) in the center, and the other was a reservoir plate cut in a rectangular design (9.6 cm × 1.1 cm × 0.15 cm) underneath the frit embedded plate. A channel space was created with PVC spacers having a tip-to-tip length of 7.2 cm in different designs and thicknesses, including a 350-μm-thick spacer with a trapezoidal shape (a triangular width of 0.80 cm at the inlet end decreasing to a width of 0.15 cm at the outlet). A regenerated cellulose membrane (MWCO 10 kDa) from Wyatt GmbH (Dernbach, Germany) was placed between the acrylic plate and the frit embedded plate. The carrier liquid used for the mAF4 separation was 10 mM ammonium bicarbonate (NH₄HCO₃) solution prepared with ultrapure (>18 MΩ cm) water and filtered with a nitrocellulose membrane filter (0.22 μm) from Millipore (Danvers, MA). A model SP930D HPLC pump and a model M720 UV detector from Young-Lin Instruments (Seoul, Korea) were used for the delivery of carrier solution to the mAF4 channel and for monitoring proteins at 280 nm, respectively. Sample injection was made via a model 7725i Rheodyne injector during the focusing/relaxation mode in which two flow streams from both the inlet and the outlet were focused at a 1/10 position from the channel inlet by converting two 3-way valves (dotted lines in Figure 1). The pump flow was divided at a ratio of 1:9 by controlling the length of the 0.010 in. i.d. Teflon tube at the inlet end from a 3-way valve and the 0.020 in. i.d. Teflon tube at the outlet. After focusing/relaxation, flow was delivered to the channel inlet only by converting the valves, and the channel outflow was set to 60 μL/min using a silica capillary tubing.

The mAF4 channel was directly interfaced with a model ELAN DRC-e ICPMS from PerkinElmer Inc. (Waltham, MA) via a cyclonic spray chamber without flow splitting, as shown in Figure 1. The carrier liquid of mAF4 separation was 10 mM ammonium bicarbonate (NH₄HCO₃) solution prepared with ultrapure (>18 MΩ cm) water, and the outflow (60 μL/min) was directly fed to the ICPMS. Operating conditions for the ICPMS were as follows: 18.0 L/min plasma gas (Ar), 1.2 L/min auxiliary gas (Ar), 0.95 L/min nebulizer gas flow rate, 1400 W ICP rf power, 7 V lens voltage, 50 ms dwell time, and 10 sweeps/reading. The elements analyzed from human plasma samples were ⁵²Cr, ⁵⁵Mn, ⁵⁷Fe, ⁵⁹Co, ⁶⁰Ni, ⁶³Cu, ⁶⁶Zn, ⁷⁵As, ⁸²Se (GPx as I.X., internal standard), ⁷⁹Br, ⁸⁸Sr, ⁹⁰Zr, ⁹³Nb, ⁹⁵Mo, ¹⁰⁷Ag, ¹²⁷I, and ¹³⁷Ba.

nLC-ESI-MS/MS. nLC-ESI-MS/MS analysis was carried out using a binary LC pump (model 1260 capillary LC system; Agilent Technologies, Waldbronn, Germany), interfaced with a LTQ Velos ion trap mass spectrometer from Thermo Finnigan (San Jose, CA) with an analytical column, which was prepared in our laboratory. Briefly, the capillary column was prepared by packing 3 μm-100 Å Magic C18AQ resin in a pulled-tip capillary (15 cm × 75 μm i.d.) without a frit. The trapping column was packed with 3 μm-200 Å Magic C18AQ in a capillary tube (2 cm × 200 μm i.d.), which was capped with a

sol-gel frit prepared in our laboratory. Details of the column preparation and assembly of the capillary column for nLC-ESI-MS/MS analysis are provided in previous studies.^{46,47} Mobile phase solutions for gradient elution were 98:2 (v/v) water/acetonitrile for A and 95:5 acetonitrile/water for B, with addition of 0.1% formic acid for both. Gradient elution for peptide separation began with 2% mobile phase B, ramped to 10% B for 1 min, gradually increased to 50% B for 59 min, increased to 80% B for 3 min, and then maintained for 10 min until the end of separation. The mobile phase B was then returned to 2% B in 2 min, and the column was allowed to re-equilibrate for 15 min. The flow rate at the column outlet was adjusted to 200 nL/min by applying a pressure capillary tube (20 μm i.d.) at a controlled length attached to the microtee located at the column inlet.

MS experiments were carried out using the following conditions: +2.5 kV ESI voltage, *m/z* 300–1800 for the precursor scan, selection of three prominent precursor ions for data-dependent MS/MS analysis for each precursor scan, and 35.0% normalized collision energy for CID experiments. MS/MS spectra were analyzed using Proteome Discoverer software (version 1.4.0.288) with the proteome database from nrNCBI. The mass tolerance values were 1.0 Da for precursor ions and 0.8 Da for fragment ions. Δ*C_n* scores of 0.1 and cross-correlation (Xcorr) values larger than 2.4, 2.8, and 3.7 for 1+, 2+, and 3+ charged ions, respectively, were used. The variable modification was set as oxidation of methionine (+ 15.99492 Da), CM (+ 58.00548 Da), and iCCM (+ 61.04073 Da) of cysteine.

Quantitative Proteomic Analysis with iCCM by nLC-ESI-MS/MS. Quantification of proteins in mAF4 fractions was carried out with nLC-ESI-MS/MS using an isotope coded carbamidomethylation (iCCM) procedure developed in a previous work.⁴⁴ Each fraction collected from the mAF4 run was accumulated after 20 repeated injections and concentrated using an Amicon Ultra Centrifugal Filter Unit (MWCO 10 kDa) from Millipore (Danvers, MA), followed by Bradford assays to determine the protein contents. Each concentrated fraction was resuspended in 0.1 M PBS containing 8 M urea and 10 mM dithiothreitol and incubated for 2 h at 37 °C. During the protection of the thiol group in Cys by alkylation, one plasma fraction from a healthy control was mixed with 20 mM IAA and one plasma fraction from a patient with cancer was mixed with 20 mM isotope-labeled IAA (¹³C₂H₂D₂INO, or IAA*). Both fractions were incubated in an ice bath for 2 h in the dark, and the remaining IAA or IAA* reagents were removed by adding cysteine (40-fold excess of IAA) and vortexing for 30 min. Samples were then diluted with 0.1 M PBS to adjust the final concentration of urea to 1 M. Both CM- and iCCM-labeled protein fractions were mixed together and digested by adding sequencing-grade trypsin and Lys-C (1/40 of target protein amount), followed by a 24 h incubation at 37 °C. Finally, each mixture was desalted using an Oasis HLB cartridge from Waters (Milford, MA), and the resulting peptide mixtures were lyophilized and stored in a freezer for nLC-ESI-MS/MS. nLC-ESI-MS/MS analysis was carried out using a binary LC pump (model 1260 capillary LC system; Agilent Technologies, Waldbronn, Germany), interfaced with an LTQ Velos ion trap mass spectrometer from Thermo Finnigan (San Jose, CA) with an analytical column prepared in our laboratory.

RESULTS AND DISCUSSION

Evaluation of mAF4-ICPMS for Metal Detection from Protein Standards. The mAF4-ICPMS method for selective detection of metals in metalloproteins is demonstrated in Figure 2. mAF4-based separation of protein standard mixtures

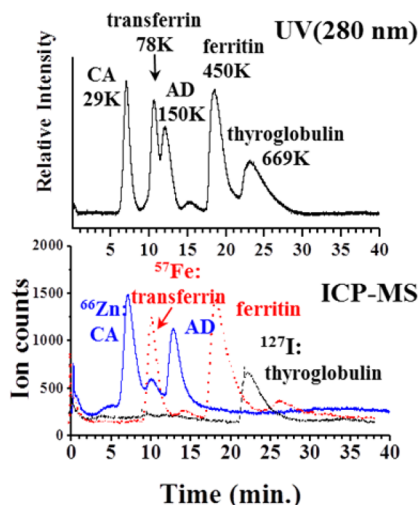


Figure 2. Separation of five protein standards (2 μg each) with mAF4-UV (top) and mAF4-ICPMS (bottom) at $\dot{V}_{\text{in}}/\dot{V}_{\text{out}} = 0.5/0.06$ mL/min. Dimer peaks of CA, transferrin, and ferritin were selectively observed with mAF4-ICPMS detection (CA, carbonic anhydrase; AD, alcohol dehydrogenase).

(2 μg of each protein) was detected by UV at 280 nm (top) and ICPMS (bottom) as follows: ^{66}Zn in carbonic anhydrase (CA) and alcohol dehydrogenase (AD), ^{57}Fe in transferrin and ferritin, and ^{127}I in thyroglobulin. Because the mAF4-ICPMS fractograms represent specific ion signals, clear separation of monomers and dimers were observed for CA, transferrin, and ferritin. By employing a miniaturized channel, the outflow rate was reduced to $\dot{V}_{\text{out}} = 60$ $\mu\text{L}/\text{min}$, which was sufficient for direct feeding to ICP without splitting flow. While the present study utilized 10 mM NH_4HCO_3 solution as a carrier liquid for mAF4, 10 mM PBS (phosphate buffered saline) solution was tested for protein separation in Figure S1 of the Supporting Information, representing that retention times of protein standards in ammonium bicarbonate solution were reduced with increased peak intensities for the late eluting ferritin and thyroglobulin due to the decreased peak broadening compared to the PBS solution. Though retention times were reduced to some degree due to the difference in ionic strengths ($I = 10$ mM vs 16 mM for PBS) of the two solutions, a loss of peak as a result of protein decomposition or an elongated retention of protein as a result of denaturation were not observed with ammonium bicarbonate solution. Since PBS solution contains a significant amount of Na which is not desirable for baseline in ICPMS, NH_4HCO_3 , which is volatile in ICP, was utilized throughout the study.

Because separation in mAF4 requires a focusing/relaxation procedure in which sample components are focused near the channel inlet prior to elution by applying counter-directing flows to ensure equilibrium conditions, any species smaller than the pore size (20 kDa) of the channel membrane will be swept through the membrane; therefore, this method can be helpful for reducing the matrix effect by removing chemical reagents or salts left in a biological sample. For analysis of blood plasma

samples, free unbound metals or small metabolites can be removed during focusing/relaxation. Figure 3 shows the

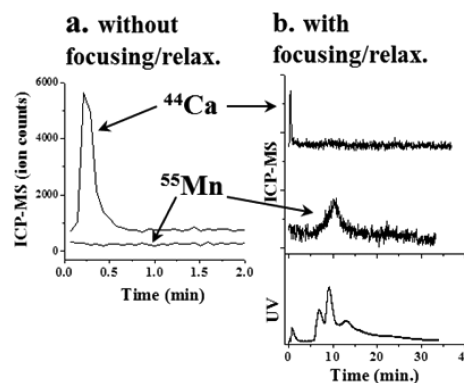


Figure 3. Comparison of element detection (^{44}Ca and ^{55}Mn) for a healthy normal plasma sample (depleted) (a) without (direct passage of plasma through mAF4 channel to ICPMS) and (b) with focusing/relaxation for size separation of plasma proteins by mAF4-ICPMS and mAF4-UV detection.

comparison of metal detection with or without applying focusing/relaxation obtained by injecting 20 μL (1 $\mu\text{g}/\mu\text{L}$ after depletion of albumin and IgG) of the depleted plasma sample (equivalent to 4 μL of the raw plasma) from a healthy normal adult to mAF4. Without focusing/relaxation and crossflow (Figure 3a), such that the components in plasma passed the channel without being retained, calcium was detected with an intense signal at the beginning of elution, while manganese was not detected during the same breakthrough run. When the focusing/relaxation procedure was applied with crossflow (Figure 3b), calcium was detected only at the beginning of the run with decreased intensity, and manganese was detected at around 10 min. This result can be explained by the observations that most of the free unbound calcium was washed off from the channel membrane and that some small calcium binding proteins (<20 kDa) were eluted with the void peak. These results may be due to the weak charge-accepting ability of calcium from the bound ligand compared with that of transition metals. However, manganese, which was not detected in the breakthrough run, was detected with mAF4-ICPMS, demonstrating the enrichment effect of focusing/relaxation for low-abundance proteins (in this case, Mn-bound proteins) in plasma without the interruption from free unbound metals that are less distinguishable in column-based analysis with ICPMS.

Metal Analysis of Human Plasma Proteins by mAF4-ICPMS. mAF4-ICPMS analysis of metalloproteins was carried out by analyzing the detection of 16 elements, including two halogens (Br and I), from depleted plasma samples of patients with lung cancer in comparison with those from healthy controls. Figure 4 shows the mAF4-ICPMS fractograms plotted for five ions between the pooled healthy normal (control, black) and a pooled lung cancer (red) plasma samples ($n = 10$ for both groups). The injection amount was the same as that used in Figure 3. In Figure 4, the intensities of ^{55}Mn and peak 1 of ^{63}Cu were significantly decreased in patient plasma; however, peak 1 (from smaller-molecular-weight [MW] proteins) of ^{66}Zn and ^{127}I (Figure 4b) showed significant increases in intensity, with a distinct decrease in the width of peak 2 of zinc. Moreover, the ^{90}Zr peak exhibited an increased retention time (from 11.00 to 12.26 min) and a broadened peak. The intensity

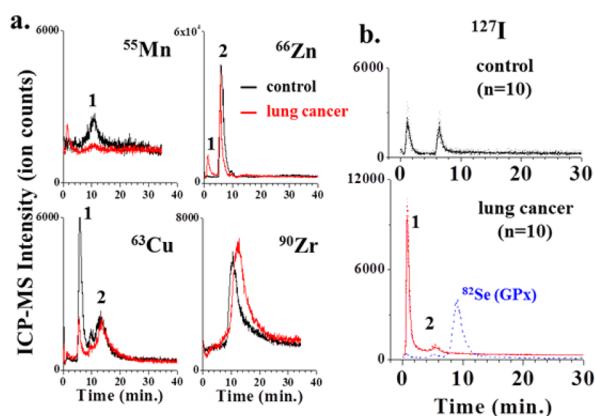


Figure 4. (a) Elemental fractograms of ^{55}Mn , ^{63}Cu , ^{66}Zn , and ^{90}Zr from metalloproteins of pooled healthy normal plasma as a control ($n = 10$, black) and pooled plasma from patients with lung cancer ($n = 10$, red) (after depletion) by mAF4-ICPMS and (b) comparison of individual peaks of ^{127}I between 10 controls and 10 patients. It was superimposed with the MS signal for ^{82}Se from GPx as an internal standard.

increases for peak 1 of zinc and iodine may represent the dissociation of a complex with associated proteins into smaller subunits. For the case of zirconia, aggregation or formation of a large complex may occur. Moreover, two metals (^{60}Ni and ^{137}Ba) exhibited only slight changes, whereas the remaining five metals (^{52}Cr , ^{57}Fe , ^{79}Br , ^{88}Sr , and ^{93}Nb) showed insignificant changes (Figure S2 in the Supporting Information). Data for four metals (^{59}Co , ^{75}As , ^{95}Mo , and ^{107}Ag) were not included since these metals were not detected. The peak variations of individual samples by mAF4-ICPMS are shown in Figure 4b, with a comparison of the detection of ^{127}I from (a) 10 samples from controls and (b) 10 samples from patients with cancer. The results from ^{63}Cu and ^{90}Zr are shown in Figure S3. For the case of ^{127}I , slight variations in the peak intensities among individuals were observed for both controls and patients. However, fractograms of ^{63}Cu -containing proteins (Figure S3a) showed some variations in peak intensities among individual samples, with obvious decreases in the first peak in samples from patients with cancer. The lower fractograms in Figure 4b were superimposed with the ^{82}Se peak from glutathione peroxidase (GPx, 84 kDa) which was added to plasma samples as an internal standard (IS; 3 μg in 20 μL of each depleted plasma sample) for the compensation of spectral fluctuations between runs. The addition of GPx to plasma samples was tested by examining the matrix effect during mAF4-ICPMS analysis, which was found to be insignificant in this study. Figure S4a shows superimposed fractograms of ^{82}Se obtained by varying the injection amount of GPx (25–150 ppm in 20 μL of the depleted plasma sample, demonstrating that the overloading was not observed and that there was good linearity ($R^2 = 0.998$) in the peak area relationship with the GPx concentration. The effects of plasma concentrations on the detection of GPx (^{82}Se) in Figure S4b demonstrated that insertion of a fixed amount (150 ppm) of GPx into the depleted plasma by varying the plasma protein concentrations (0–1000 ppm: 0–20 μg of plasma proteins in a total 20 μL injection) showed that there was a $\sim 2.5\%$ difference in the peak area of ^{82}Se . These data supported that the matrix effect from plasma proteins was not significant with using ^{82}Se as an internal standard within the concentration range.

Relative Quantification of Metalloproteins by mAF4-ICPMS. Quantification of each metal in samples from patients with lung cancer and controls was carried out by comparing peak areas from each individual sample. Quantitative comparisons between patients and controls were made by calculating the ratio of the peak area of patient to control (P/C) for the 12 elements in Table 1, and each individual peak

Table 1. Average Retention Time (t_r) and Calculated Peak Area Ratios (P/C, Cancer/Control) of Elemental Peaks from Plasma Samples from Patients with Lung Cancer to Those of Healthy Controls Obtained by mAF4-ICPMS

	t_r (min.), pooled		P/C	
	control	lung cancer	pooled	individual ($n = 10$)
^{52}Cr	5.92 ± 0.09	5.86 ± 0.26	0.99 ± 0.16	1.05 ± 0.18
	10.10 ± 0.11	10.29 ± 0.38	1.04 ± 0.13	1.21 ± 0.24
^{55}Mn	10.83 ± 0.17	10.84 ± 0.41	0.27 ± 0.05	<u>0.33 ± 0.11</u>
^{57}Fe	8.00 ± 0.19	7.72 ± 0.12	1.16 ± 0.17	0.98 ± 0.15
^{60}Ni	7.05 ± 0.13	6.89 ± 0.31	0.74 ± 0.17	<u>0.65 ± 0.19</u>
^{63}Cu	6.71 ± 0.09	6.64 ± 0.15	0.29 ± 0.08	<u>0.50 ± 0.07</u>
	13.96 ± 0.21	13.92 ± 0.09	1.33 ± 0.23	1.04 ± 0.26
^{66}Zn	1.86 ± 0.15	1.81 ± 0.35	2.65 ± 0.76	<u>2.32 ± 0.41</u>
	6.83 ± 0.16	6.77 ± 0.28	0.66 ± 0.05	<u>0.73 ± 0.06</u>
^{79}Br	6.45 ± 0.09	6.47 ± 0.25	1.07 ± 0.10	0.89 ± 0.21
^{88}Sr	10.47 ± 0.11	10.08 ± 0.15	0.96 ± 0.12	1.04 ± 0.08
^{90}Zr	11.00 ± 0.22	12.26 ± 0.47	1.21 ± 0.29	<u>1.17 ± 0.16</u>
^{93}Nb	11.99 ± 0.13	12.04 ± 0.14	0.95 ± 0.13	0.97 ± 0.09
^{127}I	0.70 ± 0.23	0.61 ± 0.15	4.35 ± 0.93	<u>5.87 ± 1.76</u>
	6.74 ± 0.22	6.50 ± 0.26	0.87 ± 0.14	1.09 ± 0.26
^{137}Ba	11.65 ± 0.12	11.04 ± 0.50	1.37 ± 0.14	<u>1.37 ± 0.26</u>

^aEach sample was measured in triplicate. The underlined P/C values showed significant difference between patients and controls ($p < 0.01$).

area value utilized for calculation was the relative peak area (versus IS) measured from each run. Differences in retention times between patient and control samples were less than 5% for most elemental peaks, except zirconia-containing proteins (11% increase in patients), as observed in Figure 4. For P/C values obtained from individual samples, most elements showed similar values between patients and controls; however, seven elements (^{55}Mn , ^{60}Ni , ^{63}Cu , ^{66}Zn , ^{90}Zr , ^{127}I , and ^{137}Ba) showed significant differences ($p < 0.01$; Table 1). Among these elements, ^{55}Mn was decreased by 3-fold, ^{60}Ni and ^{63}Cu were decreased by more than 30% in patients, ^{66}Zn and ^{127}I were increased by about 2–5-fold, and ^{137}Ba was increased by about 37%. The calculated P/C values obtained from each pooled sample did not show large differences from the average of 10 individual data for most elements, except for the first peak of copper; the reasons for this difference are not clear.

The P/C ratio in Table 1 does not reflect changes in the concentration of a single metalloprotein but rather the total change in the concentrations of several metalloproteins harboring the same metal. However, relative quantification of metals bound to plasma proteins in this study showed that there was a certain change in metalloprotein levels or the degree of metal complexation in lung cancer plasma compared with that in healthy controls, suggesting that the online use of mAF4 with ICPMS could be applied as a high-speed top-down screening method based on metals by targeting metalloproteins

exhibiting changes in specific diseases or physiological conditions.

Metalloproteomic Analysis of mAF4 Fractions Using iCCM-Based Quantification. For the qualitative and quantitative analysis of metalloproteins in lung cancer and control plasma samples (pooled samples), four fractions were collected during mAF4 separation of plasma samples. One portion of the collected protein fraction was digested and analyzed by nLC–MS/MS for protein identification. The remaining protein fractions were then used for iCCM-based quantification by nLC–MS/MS with the SRM method, using IAA for the control and IAA* for lung cancer samples. Figure 5a shows fractograms based on ICPMS (top) signals of ^{63}Cu

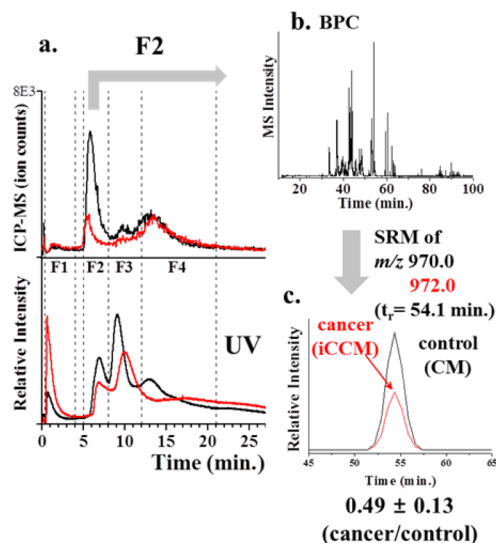


Figure 5. (a) ^{63}Cu -fractograms (top) by mAF4-ICPMS and mAF4-UV fractograms (bottom) from 10 μL plasma samples (2.5 $\mu\text{g}/\mu\text{L}$ for albumin-IgG-depleted plasma): control (black) and lung cancer (red). (b) BPC of digested peptides from F2 (5.0–8.0 min) by nLC–ESI-MS/MS. (c) Quantitative results of QTDYQQVQSc*ALPTDAL from hephaestin-like protein 1 (SRM transition of m/z 970.0 \rightarrow 567.2 for the CM-labeled b5 ion and m/z 972.0 \rightarrow 571.2 for the iCCM-labeled ion at $t_r = 54.1$ min), resulting in a P/C ratio of 0.41 ± 0.13 .

and ultraviolet (UV) spectra (bottom) from each depleted plasma sample marked with the time intervals of the may have been from proteins containing ^{127}I , as observed in Figure 4; however, quantitative results for ^{127}I were not included in Table 2 because quantification of ^{127}I -containing proteins was not successful. As shown in Table 2, the P/C ratio of Mn from mAF4-ICPMS was reduced to 0.27 ± 0.05 , consistent with the significant downregulation of the two Mn-containing proteins. Specifically, terminal uridylyltransferase 4 was not detected in cancer, and the dominant-negative kinase-deficient Brutons tyrosine kinase isoform 4 was reduced to 0.33 ± 0.08 . Peptide sequences for each protein identified are listed in Table S3. The ^{66}Zn -elemental and proteomic results showed similar trends for both F1 and F2, i.e., an increase (2.65 ± 0.76) in F1 (smaller than ~ 60 kDa) and a decrease (0.66 ± 0.05) in F2, consistent with the quantified proteomic data. All six proteins were increased in cancer samples in F1; however, four (underlined) of these six proteins were also found in F2 but not increased as much, and the remaining proteins in F2 were markedly reduced in patients with cancer. Elution of the same protein at the two different retention times in AF4 was observed when there was a

change in the hydrodynamic radius of the protein by denaturation, representative of associations with other proteins or lipoprotein complexes. The four Zn binding proteins found in the F1 fraction were increased in cancer samples; however, their peak areas from peptides were much smaller than those found in F2. By considering the MWs of these proteins (less than 60 kDa), the presence of these proteins in F2 may be explained by the formation of high-molecular-weight complexes with other proteins. However, the current experiments were not able to explain these findings.

CONCLUSIONS

In this study, we introduced mAF4-ICPMS for direct metal analysis of metalloproteins from lung cancer plasma samples and off-line coupling of mAF4 with nLC–MS/MS for the iCCM-based quantification of metalloproteins after collecting size-sorted protein fractions. Among 16 elements examined by mAF4-ICPMS, seven elements (^{55}Mn , ^{60}Ni , ^{63}Cu , ^{66}Zn , ^{90}Zr , ^{127}I , and ^{137}Ba) showed significant changes ($p < 0.01$) in lung cancer plasma compared with controls. However, quantification of metalloproteins known to associate with the examined elements showed significant changes in four metals (^{55}Mn , ^{60}Ni , ^{63}Cu , and ^{66}Zn). Although the two analytical approaches used in this study were based on different detection principles (metal concentrations versus metalloproteins), the results showed common trends, with decreased Mn, Ni, and Cu in patients with lung cancer and variations in Zn (an increase in the low-MW [$< \sim 60$ kDa] protein fraction and a decrease in the high-MW fraction). The use of mAF4 prior to ICPMS provides several advantages over other separation methods including SEC for handling proteins. Potential loss of proteins during mAF4 separation can be minimized through the use of an unobstructed channel, and conformation of metalloproteins can be maintained during separation due to the use of aqueous buffer solution. Information on metals associating with metalloproteins can be distinguished from free unbound metals, which are readily swept through the channel during separation. Impurities, including low-MW metabolites and salts contained in biological samples, can be readily removed during mAF4 separation, which may also reduce the matrix effect during metal detection. Moreover, enrichment of low-abundance proteins can be obtained during the focusing/relaxation process in the mAF4 operation, enabling detection of Mn-containing proteins when a breakthrough run of plasma with ICPMS is not successful. Changes in the retention time of metalloproteins can be monitored when there is a conformational change from the formation of metal complexes or decomplexation. The proposed method shows a potential for a rapid screening of metalloproteins related to diseases once metalloprotein biomarkers are well established. Systematic analysis of the qualitative and quantitative properties of metalloproteins together with the enhancement of metal detection from plasma samples during mAF4-ICPMS is needed. While mAF4 was employed in this evaluation study, any miniaturized FIFFF including hollow fiber FIFFF (HF5) can be utilized for the hyphenation with ICPMS once the outflow can be adjusted to a microflow rate scale.

Table 2. Comparison of Calculated Peak Area Ratios (P/C) of ^{55}Mn -, ^{63}Cu -, and ^{66}Zn -Binding Proteins from Plasma Samples Obtained by nLC–ESI-MS/MS (Using the iCCM Method) and mAF4-ICPMS Analysis

metal	nLC–ESI-MS/MS					mAF4-ICPMS	
	metal-binding proteins		MW (kDa)	peak area (10^6)		P/C	
			control	cancer	P/C	P/C	
^{55}Mn	F3, F4	Terminal uridylyltransferase 4	185	5.01	N.D.	0.33 ± 0.08	0.27 ± 0.05
		Dominant-negative kinase-deficient Brutons tyrosine kinase isoform 4	22.8	0.48	0.16		
	Threonylcarbamoyladenine tRNA methyltransferase	49.8	3.19	3.35			
	Haptoglobin	45.2	17.32	18.99			
F2	Hemopexin	51.7	4.14	5.44	1.31 ± 0.21	1.16 ± 0.17	
	Serotransferrin	77.1	17.39	19.85	1.14 ± 0.05		
^{57}Fe	F3	Hemopexin	51.7	3.00	3.28	1.09 ± 0.17	1.16 ± 0.17
		Serotransferrin	77.1	14.65	18.45	1.26 ± 0.10	
				13.88	12.97	0.93 ± 0.18	
^{60}Ni	F1	Poly(ADP-ribose) glycohydrolase	17	4.98	6.85	1.37 ± 0.35	0.74 ± 0.17
	F3	3-phosphoglycerate dehydrogenase	24.2	5.26	2.08	0.39 ± 0.05	
^{63}Cu	F1	Metallothionein	4.3	4.32	3.99	0.92 ± 0.08	1.14 ± 0.27
	F2	Metallothionein	4.3	10.86	26.09	2.44 ± 0.53	0.29 ± 0.08
		Hephaestin-like protein 1	131.6	16.36	8.04	0.49 ± 0.13	
	F4	Ceruloplasmin	115.4	7.61	8.58	1.13 ± 0.15	1.33 ± 0.23
	F1	Zinc finger protein 407	247.2	0.23	0.94	4.02 ± 0.43	2.65 ± 0.76
		Zinc finger protein 292	304.6	0.28	0.47	1.69 ± 0.11	
		Zinc finger SWIM domain-containing protein 7	15.4	0.34	0.64	1.86 ± 0.29	
		Zinc finger protein 691	34.6	N.D.	0.24		
		Acrosin	45.8	N.D.	0.32		
		Zinc transporter 1	55.3	0.41	0.65	1.58 ± 0.36	
^{66}Zn	F2	Zinc finger SWIM domain-containing protein 7	15.4	2.75	2.61	0.95 ± 0.16	0.66 ± 0.05
		Zinc finger protein 691	34.6	1.26	1.58	1.25 ± 0.18	
		Acrosin	45.8	3.92	5.16	1.32 ± 0.09	
		Zinc transporter 1	55.3	2.36	2.32	0.98 ± 0.12	
		Zinc finger with UFM1-specific peptidase domain protein	65.9	0.45	0.32	0.71 ± 0.08	
		E3 ubiquitin-protein ligase BRE1A	113.6	1.48	1.31	0.88 ± 0.20	
		CXXC-type zinc finger protein 4	21.0	0.42	0.26	0.61 ± 0.14	
		Zinc finger protein 490	61.3	13.38	13.81	1.03 ± 0.31	
ADAMTS-like protein 2	104.6	0.44	0.24	0.54 ± 0.02			
ZFH3 protein	98.5	1.27	1.42	1.12 ± 0.18			
Arf-GAP with coiled-coil, ANK repeat and PH domain-containing protein 2	88	0.45	0.38	0.85 ± 0.08			
Zinc-alpha-2-glycoprotein	34.2	8.39	12.14	1.45 ± 0.23			

^aEach sample was measured in triplicate.

■ ASSOCIATED CONTENT

📄 Supporting Information

The Supporting Information is available free of charge on the ACS Publications website at DOI: 10.1021/acs.analchem.6b02775.

Data of mAF4 operation, additional nLC–ESI-MS/MS spectra, matrix effect of GPx during mAF4-ICPMS, list of 327 proteins identified by nLC–ESI-MS/MS from mAF4 fractions, list of 58 metalloproteins identified from the Uniprot Knowledgebase and classified according to metals, and quantification results of metal-

loproteins represented as the peak area ratio (P/C) for each peptide quantified by nLC–ESI-MS/MS using iCCM (PDF)

■ AUTHOR INFORMATION

Corresponding Authors

*Phone: (82) 31 8005 3151. Fax: (82) 31. E-mail: plasma@dankook.ac.kr.

*Phone: (82) 2 2123 5634. Fax: (82) 2 364 7050. E-mail: mhmoon@yonsei.ac.kr.

Notes

The authors declare no competing financial interest.

ACKNOWLEDGMENTS

This study was supported by a grant (Grant NRF-2015SR1A2A1A01004677) from the National Research Foundation of Korea.

REFERENCES

- (1) Waldron, K. J.; Rutherford, J. C.; Ford, D.; Robinson, N. J. *Nature* **2009**, *460*, 823–839.
- (2) Lu, Y.; Yeung, N.; Sieracki, N.; Marshall, N. M. *Nature* **2009**, *460*, 855–862.
- (3) Roberts, E. A.; Sarkar, M. *Curr. Opin. Clin. Nutr. Metab. Care* **2014**, *17*, 425–430.
- (4) Rowinska-Zyrek, M.; Salerno, M.; Kozlowski, H. *Coord. Chem. Rev.* **2015**, *284*, 298–312.
- (5) Eskici, G.; Axelsen, P. H. *Biochemistry* **2012**, *51*, 6289–6311.
- (6) Chen, J.; Marks, E.; Lai, B.; Zhang, Z.; Duce, J. A.; Lam, L. Q.; Volitakis, I.; Bush, A. I.; Hersch, S.; Fox, J. H. *PLoS One* **2013**, *8*, e77023.
- (7) Fatemi, N.; Sarkar, B. *Inorg. Chim. Acta* **2002**, *339*, 179–187.
- (8) Stadler, N.; Lindner, R. A.; Davies, M. J. *Arterioscler., Thromb., Vasc. Biol.* **2004**, *24*, 949–954.
- (9) Yaman, M.; Atici, D.; Bakirdere, S.; Akdeniz, I. *J. Med. Chem.* **2005**, *48*, 630–634.
- (10) Hua, Y.; Clark, S.; Ren, J.; Sreejayan, N. *J. Nutr. Biochem.* **2012**, *23*, 313–319.
- (11) Salnikow, K.; Zhitkovich, A. *Chem. Res. Toxicol.* **2008**, *21*, 28–44.
- (12) Leonard, S. S.; Bower, J. J.; Shi, X. *Mol. Cell. Biochem.* **2004**, *255*, 3–10.
- (13) Lobinski, R.; Becker, J. S.; Haraguchi, H.; Sarkar, B. *Pure Appl. Chem.* **2010**, *82*, 493–504.
- (14) Prange, A.; Pröfrock, D. *Anal. Bioanal. Chem.* **2005**, *383*, 372–389.
- (15) Haider, S. R.; Sharp, B. L.; Reid, H. J. *TrAC, Trends Anal. Chem.* **2011**, *30*, 1793–1808.
- (16) Hu, B.; Peng, L.; He, M.; Chen, B. *Appl. Spectrosc. Rev.* **2016**, *51*, 94–116.
- (17) Yin, X.-B.; Li, Y.; Yan, X.-P. *TrAC, Trends Anal. Chem.* **2008**, *27*, 554–565.
- (18) Timerbaev, A. R. *Chem. Rev.* **2013**, *113*, 778–812.
- (19) Manley, S. A.; Gailer, J. *Expert Rev. Proteomics* **2009**, *6*, 251–265.
- (20) Jara-Biedma, R.; Gonzalez-Dominguez, R.; Garcia-Barrera, T.; Lopez-Barea, J.; Pueyo, C.; Gomez-Ariza, J. L. *BioMetals* **2013**, *26*, 639–650.
- (21) Lobinski, R.; Chassaing, H.; Szpunar, J. *Talanta* **1998**, *46*, 271–289.
- (22) Vogiatzis, C. G.; Zachariadis, G. A. *Anal. Chim. Acta* **2014**, *819*, 1–14.
- (23) Infante, H. G.; Sanchez, M. L. F.; Sanz-Medel, A. *J. Anal. At. Spectrom.* **1999**, *14*, 1343–1348.
- (24) Miyayama, T.; Ogra, Y.; Suzuki, K. T. *J. Anal. At. Spectrom.* **2007**, *22*, 179–182.
- (25) Cao, Z. Y.; Sun, L. H.; Mou, R. X.; Zhou, R.; Zhu, Z. W.; Chen, M. X. *J. Chromatogr. B: Anal. Technol. Biomed. Life Sci.* **2015**, *976*, 19–26.
- (26) Giddings, J. C. *Anal. Chem.* **1981**, *53*, 1170A–1175A.
- (27) Giddings, J. C. *Science* **1993**, *260*, 1456–1465.
- (28) Nilsson, M.; Wahlund, K.-G.; Bulow, L. *Biotechnol. Tech.* **1998**, *12*, 477–480.
- (29) Lee, H.; Williams, S. K.; Wahl, K. L.; Valentine, N. B. *Anal. Chem.* **2003**, *75*, 2746–2752.
- (30) Reschiglian, P.; Zattoni, A.; Roda, B.; Cinque, L.; Melucci, D.; Min, B. R.; Moon, M. H. *J. Chromatogr. A* **2003**, *985*, 519–529.
- (31) Park, I.; Paeng, K.-J.; Yoon, Y.; Song, J.-H.; Moon, M. H. *J. Chromatogr. B: Anal. Technol. Biomed. Life Sci.* **2002**, *780*, 415–422.
- (32) Rambaldi, D. C.; Zattoni, A.; Casolari, S.; Reschiglian, P.; Roessner, D.; Johann, C. *Clin. Chem.* **2007**, *53*, 2026–2029.
- (33) Barman, B. N.; Ashwood, E. R.; Giddings, J. C. *Anal. Biochem.* **1993**, *212*, 35–42.
- (34) Kang, D.; Oh, S.; Reschiglian, P.; Moon, M. H. *Analyst* **2008**, *133*, 505–515.
- (35) Kang, D.; Oh, S.; Ahn, S.-M.; Lee, B. H.; Moon, M. H. *J. Proteome Res.* **2008**, *7*, 3475–3480.
- (36) Kim, K. H.; Moon, M. H. *Anal. Chem.* **2011**, *83*, 8652–8658.
- (37) Byeon, S. K.; Kim, J. Y.; Lee, J. Y.; Chung, B. C.; Seo, H. S.; Moon, M. H. *J. Chromatogr. A* **2015**, *1405*, 140–148.
- (38) Murphy, D. M.; Garbarino, J. R.; Taylor, H. E.; Hart, B. T.; Beckett, R. J. *Chromatogr.* **1993**, *642*, 459–467.
- (39) Hasselov, M.; Lyven, B.; Haraldsson, C.; Sirinawin, W. *Anal. Chem.* **1999**, *71*, 3497–3502.
- (40) Dubascoux, S.; Hecho, I. L.; Hasselov, M.; Kammer, F. V. D.; Gautier, M. P.; Lespes, G. *J. Anal. At. Spectrom.* **2010**, *25*, 513–623.
- (41) M-M, P.; Siripinyanond, A. *J. Anal. At. Spectrom.* **2014**, *29*, 1739–1752.
- (42) Siripinyanond, A.; Barnes, R. M. *J. Anal. At. Spectrom.* **1999**, *14*, 1527–1531.
- (43) Loeschner, K.; Harrington, C. F.; Kearney, J.-L.; Langton, D. J.; Larsen, E. H. *Anal. Bioanal. Chem.* **2015**, *407*, 4541–4544.
- (44) Kim, J. Y.; Oh, D.; Kim, S.-K.; Kang, D.; Moon, M. H. *Anal. Chem.* **2014**, *86*, 7650–7657.
- (45) Yang, I.; Kim, K. H.; Lee, J. Y.; Moon, M. H. *J. Chromatogr. A* **2014**, *1324*, 224–230.
- (46) Kim, J. Y.; Kim, S.-K.; Kang, D.; Moon, M. H. *Anal. Chem.* **2012**, *84*, 5343–5350.
- (47) Kim, J. Y.; Lee, S. Y.; Kim, S.-K.; Park, S. R.; Kang, D.; Moon, M. H. *Anal. Chem.* **2013**, *85*, 5506–5513.